Subtilase SBT5.2 inactivates flagellin immunogenicity in the plant apoplast

Pierre Buscaill[1,4], Nattapong Sanguankiattichai[1], Farnusch Kaschani[2], Jie Huang[1], Brian C. Mooney[1], Yuge Li[1,3], Joy Lyu[1], Daniela Sueldo[1,5], Markus Kaiser[2] and Renier A. L. van der Hoorn[1*]

[1] The Plant Chemetics Laboratory, Department of Biology, University of Oxford, OX1 3RB, Oxford, United Kingdom

[2] ZMB Chemical Biology, Faculty of Biology, University of Duisburg-Essen, Essen, Germany

[3] Guangdong Provincial Key Laboratory of Applied Botany and State Key Laboratory of Plant Diversity and Prominent Crops, South China Botanical Garden, Chinese Academy of Sciences, Guangzhou 510650, China.

[4] Current address: School of Biological Sciences, University of Bristol, BS8 1TQ, Bristol, United Kingdom

[5] Current address: Department of Biology, Norwegian University of Science and Technology, Trondheim, Norway

***Corresponding author**: renier.vanderhoorn@biology.ox.ac.uk

Abstract

Most angiosperm plants recognise the flg22 epitope in bacterial flagellin via homologs of cell surface receptor FLS2 and mount pattern-triggered immune responses. However, flg22 is buried within the flagellin protein indicating that proteases might be required for flg22 release. Here, we demonstrate the extracellular subtilase SBT5.2 not only releases flg22, but also inactivates the immunogenicity of flagellin and flg22 by cleaving within the flg22 epitope, consistent with previous reports that flg22 is unstable in the apoplast. The prolonged lifetime of flg22 in *sbt5.2* mutant plants results in increased bacterial immunity in priming assays, indicating that SBT5.2 counterbalances flagellin immunogenicity to provide spatial-temporal control and restrict costly immune responses and that bacteria take advantage of the host proteolytic machinery to avoid detection by flagellin having a protease-sensitive flg22 epitope.

Keywords: Plant immunity, *Pseudomonas syringae*, flagellin, subtilases, flg22, *Nicotiana benthamiana*.

Introduction

Bacterial flagellin is a strong inducer of innate immune responses in both plants and animals. The flagellum enables bacterial motility and is a polymer that consists of thousands of flagellin proteins in a tubular assembly[1-4]. The surface of the flagellum is glycosylated with *O*-glycans that can differ in composition between bacterial strains[5].

In most angiosperms, recognition of bacterial flagellin is mediated by a cell surface localised receptor kinase called FLS2 (flagellin sensing-2[6]). FLS2 recognizes a highly conserved epitope of 22-amino acids in the N-terminal region of flagellin, called flg22[7,8]. The flg22 peptide is routinely used to trigger pattern-triggered immunity (PTI), but how flg22 is made available during infection is not yet clear.

It has been predicted that to expose flg22, the flagellin protein needs to be processed from its monomeric precursor because the flg22 epitope is not fully exposed in the flagellin monomer, and is unlikely to bind the FLS2 receptor in this conformation[9]. Indeed, a protease inhibitor cocktail can suppress the perception of flagellin, but not of flg22[10]. A recent report describes that Arabidopsis subtilases SBT5.2 and SBT1.7 are processing flagellin at the C-terminus of flg22[11]. However, despite the reduced processing of flagellin in *sbt5.2/sbt1.7* mutants, these mutants only show a 2-minute delay in the maximum release of reactive oxygen species (ROS). And although a hampered flagellin perception should have caused an increased bacterial susceptibility, increased bacterial growth on *sbt5.2/sbt1.7* mutants has not been reported.

Here, we describe how flagellin is quickly inactivated in the apoplast of the model plant *Nicotiana benthamiana* by subtilase SBT5.2 and other proteases. In addition to processing flg22 from its precursor, SBT5.2 quickly inactivates the immunogenic activity of flagellin by cleaving in the middle of the flg22 epitope. Indeed, *sbt5.2* mutants show an increased stability of flagellin and flg22 in the apoplast, associated with prolonged immunogenicity. Consequently, *sbt5.2* mutants are less susceptible to bacterial colonisation when primed with low flg22 concentrations, indicating that SBT5.2 provides spatial-temporal control over immune responses to restrict the induction of costly defence responses and that pathogens take advantage of the host proteolytic machinery by exposing protease-sensitive epitopes.

RESULTS

Flagellin monomer is immunogenic but its polymer is not

To study the processing of flagellin in the apoplast, we isolated flagella from *Pseudomonas syringae* pv. *tabaci* 6605 (*Pta*6605) to obtain polymeric flagellin that we monomerized by heat-treatment (10 min. 70 °C). To confirm the monomerization, we used a 100 kDa molecular weight cut-off filter (MWCO). Polymeric flagellin was unable to pass the 100 kDa MWCO filter, in contrast to monomeric flagellin (**Fig. 1a**). We next tested if polymeric flagellin (sample a) and monomeric flagellin (sample b) could trigger an oxidative burst in leaf discs from 4-week-old *Nicotiana benthamiana* floating on a solution containing luminol and horse radish peroxidase (HRP). Only monomeric flagellin triggered a burst of reactive oxygen species (ROS) and polymeric flagellin did not (**Fig. 1b**), demonstrating that only monomeric flagellin is recognised. Furthermore, monomerised flagellin did not trigger an oxidative burst in leaf discs of *fls2* mutant *N. benthamiana* plants[12] (**Fig. 1c**), demonstrating that the detected oxidative burst is caused by flagellin recognition via its FLS2 receptor and that no other elicitors are present in the purified flagellin samples.

Flagellin monomer is quickly degraded in AF but its polymer not

To investigate flagellin processing by apoplastic proteases, we incubated the flagellin polymer and monomerised flagellin with apoplastic fluid (AF) isolated from *N. benthamiana* and separated the proteins on protein gels to monitor the degradation of flagellin in AF over time. Monomeric flagellin rapidly degrades in AF within minutes, whereas polymeric flagellin remains stable in AF for over 24 hours (**Fig. 1d**), consistent with the hypothesis that polymeric flagellin is protected from degradation. ROS assays with these samples

revealed that the oxidative burst quickly disappears when flagellin is incubated with AF for 30 or 60 minutes (**Fig. 1e**), indicating that the immunogenicity of monomerised flagellin quickly disappears in the apoplast.

Flagellin is degraded by apoplastic proteases

To further investigate flagellin processing in AF, we precipitated the proteins with 80% acetone and analysed the peptides in the supernatant by liquid chromatography-tandem mass spectrometry (LC-MS/MS) to detect the peptides released from flagellin when incubated in AF[10]. We identified a total of 466 different flagellin-derived peptides, spanning the entire protein sequence except for peptides containing the six *O*-glycosylation sites of flagellin (Supplemental **Table S1**, **Fig. 2a)**, indicating that monomeric flagellin is not fully deglycosylated before it is processed into peptides. Indeed, peptides covering this region were detected upon incubation of nonglycosylated flagellin from the flagellin glycosyl transferase mutant *Δfgt1*[13] when incubated in AF (Supplemental **Table S2**, Supplemental **Fig. S1**),

The detected peptides released from *Pta*6605 flagellin assemble into seven clusters (**Fig. 2a,** purple line). This peptide distribution pattern suggests that flagellin undergoes cleavage at specific sites by endopeptidases and that exopeptidases subsequently remove residues from the N- and C-termini.

Closer inspection of the protein coverage indicates that flagellin might be cleaved by endopeptidase(s) at LSTS↓M↓TRLS, LQIA↓TKITS↓QIRGQT↓MAIK, ILQR↓MREL↓AV↓QSRN and EFRA↓M↓SSEL (**Fig. 2a**), of which the first two processing sites would release flg22 from its precursor.

Because we detect a loss of immunogenicity of flagellin, we also searched for putative processing sites within the flg22 sequence and found two candidate regions: LKIN↓SAKD, SAKD↓DAAG (**Fig. 2b,** inset). Processing in either of these sites would inactivate the elicitor activity[7]. Collectively, the putative cleavage sites do not have an obvious consensus sequence.

We next mapped the putative cleavage sites onto a model of the structure of the flagellin monomer. The putative cleavage sites distribute over the hinge region and various positions in α-helixes that are not exposed in polymeric glycosylated flagellin (**Fig. 2b**), explaining why monomeric flagellin is more susceptible to proteolysis than polymeric flagellin.

To confirm the cleavage events within flagellin, we designed and custom-synthesised quenched peptides (QPs) containing different cleavage sites, flanked by an N-terminal quencher (DABCYL) and a C-terminal fluorophore (Glu-EDANS). Processing these peptides releases a fluorophore that is detected by fluorescence (**Fig. 2c**). The QPs cover the two sites within flg22 (LKIN↓SAKD (QP2) and SAKD↓DAAG (QP3)); the flg22-flanking sites STSM↓TRLS (QP1) and LQIA↓TKITS (QP4), as well as one additional obvious putative processing site following the flg22 sequence (RGQT↓MAIK (QP5)). Incubation of these QPs in AF causes a rapid increase of fluorescence when compared to the water control (**Fig. 2d**), indicating that these peptides are cleaved in AF. These data also indicate that QP2 is most efficiently cleaved in AF compared to the other four QPs.

Flagellin is processed by apoplastic subtilases

To identify the class of proteases responsible for processing flagellin, we isolated AFs from leaves overexpressing protease inhibitors Epi1, *Sl*Cys8 and *Hs*TIMP, which inhibit subtilases (SBTs), papain-like Cys proteases (PLCPs) and metalloproteases, respectively[14-16]. Incubation of these AFs with quenched peptides revealed that Epi1 blocks processing of all QPs, whereas *Hs*TIMP only suppresses QP3 processing and *Sl*Cys8 and had no effect (**Fig. 3a**). QP1 processing is less efficiently blocked by Epi1, indicating that this site is cleaved by a protease different from an Epi1-sensitive subtilase. The near complete blockage of QP4 processing by Epi1 indicates that only subtilases cleave at this region. Processing of QP3 is suppressed more by Epi1 than by *Hs*TIMP, again indicating that QP3 is processed by subtilases rather than other proteases. These results indicate that subtilases are responsible for most of the flagellin processing in AF.

We next tested if Epi1 can reduce the inactivation of immunogenicity in AF by incubating flagellin or flg22 in AF for 40 minutes and measuring their ability to trigger the oxidative burst. Importantly, immunogenic activity was detected after incubation of flagellin or flg22 peptide with AFs isolated from leaves transiently expressing Epi1, but not from the EV control (**Fig. 3b**), indicating that subtilases are responsible for degrading the immunogenicity of both flagellin and flg22.

Flagellin processing requires SBT5.2 subtilases

The *N. benthamiana* genome encodes for 72 putative subtilases[17,18]. Among the ten subtilases detected in the apoplast, four are notably more abundant: SBT5.2a, SBT1.9a, SBT1.7a, and SBT1.7c[15,18,19], also referred to as SBT1-4, respectively[20]. To identify the subtilase responsible for flagellin processing, we depleted transcripts of these four subtilases using Virus-Induced Gene Silencing (VIGS) with Tobacco Rattle Virus (TRV) vectors carrying 300 bp fragments targeting these subtilases. Each fragment was designed to target one subtilase, except for the fragment present in *TRV::SBT5.2*, which targets the three *SBT5.2* homologs (*a-c*) for which transcripts were detected in *N. benthamiana*[18] (Supplemental **Fig. S2**).

To determine which subtilases are required for processing the quenched peptides, QPs were incubated with AFs isolated from *TRV::SBT* plants and fluorescence was measured. Processing of all QPs except QP1 was significantly reduced in the AF of *TRV::SBT5.2* plants compared to the *TRV::GFP* control (**Fig. 4a**). The absence of reduced QP1 processing is consistent with the observation that QP1 processing is also less sensitive to inhibition by Epi1 and indicates that QP1 is not processed by abundant, Epi1-sensitive subtilases. QP3 processing is not as strongly reduced in *TRV::SBT5.2* plants compared to the other QPs, whereas QP3 processing was also reduced in AF isolated from *TRV::SBT1.9a* and *TRV::SBT1.7a* plants. This is consistent with SBT1.9a being a phytaspase[17,21], which prefer cleaving after aspartic residues present in QP3 (SAKDDAAG). Taken together, these results indicate that SBT5.2s are responsible for processing QPs 2-5 but QP3 is also cleaved by phytaspase SBT1.9a and SBT1.7a.

Since SBT5.2s seem responsible for processing flg22 at sites 2 and 3, we tested the stability of flg22 immunogenicity by incubating flg22 for various times in AF isolated from *TRV::SBT5.2* and *TRV::GFP* plants. Importantly, the decline of flg22 immunogenicity is much slower in AF of *TRV::SBT5.2* plants compared to *TRV::GFP* plants (**Fig. 4b**), indicating that SBT5.2s are responsible for inactivating flg22.

Flagellin/flg22 is stabilised in AF of *sbt5.2* plants

To further investigate the role of SBT5.2 in flagellin processing, we took advantage of two recently described *sbt5.2* triple mutant lines of *N. benthamiana*, which are disrupted in the open reading frames encoding all three *SBT5.2* genes[18]. Activity-based profiling with FP-TAMRA on AF demonstrates that the *sbt5.2* mutants lack the most active subtilases at 70 kDa (**Fig. 5a**), consistent with being the most active subtilase in AF of *N. benthamiana*[15,19,20].

Processing of QP1, QP2 and QP5 is significantly reduced in AF of *sbt5.2* mutant plants (**Fig. 5b**). QP3 processing is only slightly reduced in AF of *sbt5.2* mutant plants, whereas QP4 processing is strongly reduced but not significant (**Fig. 5b**), However, all QPs are still cleaved to some extent in the absence of *sbt5.2*, suggesting that other proteases in AF might slowly process these peptides in the absence of SBT5.2s.

Consistent with flagellin protein degradation, the flg22 peptide retains immunogenicity significantly longer when incubated in AF isolated from *sbt5.2* plants, whereas flg22 immunogenicity is quickly lost when incubated with AF of WT plants (**Fig. 5c**).

Incubation of monomerised flagellin with AF isolated from WT and *sbt5.2* mutant plants and revealed that flagellin was more stable in the AF of both *sbt5.2* mutants than in the AF of WT plants (**Fig. 5d**), demonstrating robustly that SBT5.2s are necessary for flagellin processing. Interestingly, in addition to the full length flagellin protein we also detect the accumulation of several intermediate flagellin degradation products in AF of *sbt5.2* plants, suggesting that other proteases slowly process flagellin in the absence of SBT5.2s.

We next monitored the timing of the oxidative burst triggered by flagellin monomers in leaf discs of WT and *sbt5.2* mutants, to compare to the recently reported 2-minute delay in the peak of the ROS burst in the Arabidopsis *sbt5.2/sbt1.7* mutant[11]. In our assay, however, both the timing and the amplitude of the oxidative burst upon adding flagellin are similar between WT and *sbt5.2* mutant plants (**Fig. 5e**). Statistical analysis of the peak times did not reveal a significant difference between WT and *sbt5.2* mutant *N. benthamiana* (**Fig. 5f**). These data indicate that flagellin processing by SBT5.2 does not affect flagellin recognition. ROS responses to various flg22 concentrations are also indistinguishable between leaf discs of WT and *sbt5.2* mutant *N. benthamiana* (**Fig. 5g** and Supplemental **Fig. S3**), indicating that when added to leaf discs, flg22 is not inactivated by SBT5.2, possibly because the SBT5.2 is diluted in the medium.

Purified SBT5.2 processes flagellin and flg22

To determine if SBT5.2 is sufficient for processing QPs and flagellin and inactivating flg22, we purified SBT5.2a-His from agroinfiltrated plants using Nickel-NTA agarose[22], and used activity-based labeling with FP-TAMRA to confirm that this is active (Supplemental **Fig. S4a**). Transiently expressed secreted GFP-His was included as a negative control (Supplemental **Fig. S4b**). Incubation of these purified proteins with the QPs revealed that all QPs are substrates of SBT5.2a-His, and that QP2 is the best substrate and that QP3 is hardly cleaved, whereas no substrate is cleaved in the GFP-His control (**Fig. 6a**). Furthermore, incubation of flg22 with purified SBT5.2a-His inactivated its elicitor activity (**Fig. 6b**). Incubation of monomerised flagellin with purified SBT5.2-His caused a quick degradation of flagellin in contrast to the purified GFP-His control (**Fig. 6c** and Supplemental **Fig. 5**). The peptides released from flagellin by purified SBT5.2-His were identified by

LC-MS/MS and confirm that SBT5.2a-His cleaves at site-1, -2 and -4-7 but not at site-3 (**Fig. 6d** Supplemental **Table S3**). The few flagellin-derived peptides detected in the GFP-His control were also detected upon incubation of flagellin in water (Supplemental **Table S3**, Supplemental **Fig. S6**). Besides peptides resulting from the cleaved flg22 epitope, also a flg22 peptide was detected (**Fig.6d**), suggesting that purified SBT5.2a-His can also release flg22 from the precursor before it is inactivated. Taken together, these data demonstrate that purified SBT5.2a-His preferably cleaves QP2, inactivates flg22 immunogenicity, quickly degrades flagellin releasing peptides of the cleaved flg22 epitope.

SBT5.2s dampen flg22-induced immune responses

To determine the outcome of SBT5.2 depletion on bacterial growth, we performed infection assays on plants depleted for subtilases with *Pseudomonas syringae*. Bacterial growth on leaves transiently expressing Epi1 is significantly reduced (**Fig. 7a**), indicating that subtilases might collectively reduce the immunogenicity of flagellin or act in immune signaling. However, bacterial growth was unaltered in *TRV::SBT5.2* compared to control plants (**Fig. 7b**), and in *sbt5.2* mutant lines compared to WT plants (**Fig. 7c**).

The absence of bacterial growth phenotypes on the *sbt5.2* mutant, despite the prolonged stability of flagellin and flg22 in these mutants, prompted us to test if priming by higher flg22 levels can induce immune responses that can be detected in bacterial growth assays. Strong effects on bacterial growth are normally shown by pre-treating (priming) tissues with 1,000 nM flg2[28,23]. We reasoned that the effect of SBT5.2 depletion could only be shown at threshold flg22 concentrations because higher concentrations would trigger antibacterial immunity irrespective of SBT5.2. We therefore monitored bacterial growth in leaves pre-treated with 1, 10 and 100 nM flg22. As expected, pre-treatment of WT plants with 100 nM flg22 reduces bacterial growth compared to pre-treatments with 1 and 10 nM flg22, indicating that these low flg22 concentrations are below the threshold to induce antibacterial immunity (**Fig. 7d**). In both *sbt5.2* mutants, however, pre-treatment with 10 nM flg22 reduces bacterial growth whereas no altered bacterial growth was detected upon pre-treatment with 1 and 100 nM flg22 (**Fig. 7d**). Further experiments showed that antibacterial immunity is reduced in *sbt5.2* mutant plants also upon pre-treatment with 5 nM flg22, but not with 20 nM flg22 (Supplemental **Fig. S7**). These data demonstrate that SBT5.2 dampens antibacterial immunity by inactivating the immunogenicity of flg22 at low flg22 concentrations.

Discussion

Flagellin and flg22 are almost universally recognized by angiosperm plants. Here, we demonstrated that extracellular SBT5.2 subtilases mediate the quick inactivation of the immunogenicity of both flg22 and flagellin by cleaving in the middle of the flg22 sequence. The increased stability of flg22 in *sbt5.2* mutant plants reduces bacterial growth at low flg22 concentrations, suggesting that SBT5.2 contributes to a spatial-temporal dampening of immunity to restrict the immune responses to the infection site. We also demonstrate that abundant apoplastic subtilases are responsible for these and other flagellin processing events and that the polymeric flagellin is protease resistant.

We demonstrated that flagellin monomers are sensitive to proteolysis in apoplastic fluids in contrast to the flagellin polymers, which are stable. This is consistent with the notion that the discovered processing sites in flagellin monomers are concealed in the polymer. The only solvent-exposed regions of flagellin within the polymer are covered with *O*-glycans, which are thought to protect the polymer against proteases[10,13]. Because the flg22 epitope is concealed within the flagellin polymer, monomeric flagellin is essential for perception. Monomeric flagellin can have different sources. First, monomeric flagellin is produced in the bacterial cell and kept unfolded through its interaction with its chaperone FliS[24]. This pre-polymerised flagellin could escape into the apoplast, similar to cytoplasmic EF-Tu and CSP proteins that are also perceived in the apoplast[24,25]. Second, some flagellin monomers may fail to polymerise when secreted through the flagellin tubule during flagella synthesis but most of this leakage is prevented by the flagellin cap protein, FliD[26]. Indeed, the *fliD* mutant of *Pta*6604 secreted large amounts of monomeric flagellin and triggers strong immune responses[27]. Third, flagella are shed upon starvation and during the cell cycle[26,28-30], and although flagella do not depolymerise[31], they might release monomers when incubated in an apoplastic environment. Indeed, incubation of flagellin in apoplastic fluids containing BGAL1, which removes the terminal mVio residue from the flagellin glycan, releases more immunogenic flagellin fragments[10], indicating that BGAL1 might promote flagellin depolymerisation.

Our data indicates that cleavage site-1 and site-4 would release immunogenic flagellin fragments from flagellin. N-terminal processing of flg22 at site-1 is suppressed by subtilase inhibitor Epi1 but is not significantly suppressed when silencing *SBT5.2, SBT1.9,* or *SBT1.7s*. Site-1 processing is, however, significantly reduced in the *sbt5.2* mutant and purified SBT5.2a-His can cleave QP1, indicating that SBT5.2 can process flagellin at the N-terminal site of the flg22 epitope. C-terminal processing at site-4 is suppressed by Epi1 and upon silencing *SBT5.2*. Site-4 processing is also reduced in the *sbt5.2* mutant, although not significantly, and purified SBT5.2a-His can cleave QP4. Taken together, these data indicate that SBT5.2 could cleave flagellin at both ends of flg22 and release flg22 from its precursor. These observations are similar to the recent report that SBT5.2 in Arabidopsis processes at site-4 in the flagellin of *Pseudomonas syringae* pv. *tomato* DC3000 (*Pto*DC3000)[11]. However, we did not detect a two-minute delay in the flagellin-triggered ROS response in the *sbt5.2* mutant, in contrast to the recent study with the Arabidopsis *sbt5.2/sbt1.7* mutant[11].

Besides releasing flg22, our data indicates that flagellin is quickly processed by subtilases cleaving at site-2 and site-3 in the flg22 epitope. This is consistent with the fact that we did not detect the full length flg22 immunogenic peptides in apoplastic fluids with LC-MS/MS. Site-2 (LKIN↓SAKD) is mostly cleaved by SBT5.2 because processing of QP2 is drastically reduced upon *SBT5.2* silencing and in *sbt5.2* mutants. QP2 is also a very good substrate of purified SBT5.2a-His. Site-3 processing is probably mostly caused by SBT1.9 and SBT1.7a because QP3 processing is significantly reduced upon silencing *SBT1.9* and *SBT1.7a*. QP3 is not efficiently processed by purified SBT5.2a-His, is not significantly reduced in *sbt5.2* mutants, and not cleaved by purified SBT5.2a-His, indicating that at this site is not preferred by SBT5.2. Processing at site-3 (SAKD↓DAAG) by SBT1.9 is consistent with its annotation as a phytaspase, which cleave after Asp residues[21]. Interestingly, the recent description of flagellin processing in Arabidopsis seedling exudates indicates that flagellin of *Pto*DC3000 is also processed at site-2 and that this is reduced in seedling exudates of *sbt5.2/sbt1.7*

mutants[11], indicating that processing of flagellin within the flg22 epitope might occur universally. Indeed, we detected the same site-2 processing with apoplastic fluids from tomato (Supplemental **Table S4**, Supplemental **Fig. S8**), indicating that flagellin processing within the flg22 epitope will occur in many plant species.

Our data indicates that site-2 is preferentially cleaved within flagellin because QP2 is preferentially processed in apoplastic fluids (**Fig. 2c**) and by purified SBT5.2a-His (**Fig. 6a**). The preferred processing at site-2 is also supported by modelling of flagellin with SBT5.2a by AlphaFold Multimer (AFM[32]). The best model predicts that the catalytic Ser residue is proximate to the site-2 cleavage site such that the S2 and S4 substrate binding pockets in SBT5.2a are occupied by Ile38 (P2) and Leu36 (P4) of flagellin, respectively (Supplemental **Fig. S9**). Interestingly, this AFM model indicates that the flagellin monomer could fold on the flg22 hinge to expose this processing site to SBT5.2a (Supplemental **Fig. S9**).

The quick inactivation of flagellin and flg22 by SBT5.2 cleaving within the flg22 epitope counterbalances the perception of flagellin and flg22 (**Fig. 8**). The perception of both flagellin and flg22 in *N. benthamiana* indicates that at least some unprocessed flagellin/flg22 must have reached FLS2 and activated PTI signalling. The perception of flagellin/flg22 by FLS2 is possibly mediated by a high affinity for binding FLS2, indicating that sufficient flagellin/flg22 can bind FLS2 before being cleaved. One caveat in these studies is that the preparation of flagellin monomer includes a heat or low-pH treatment, which might denature flagellin and expose flg22.

Importantly, flagellin protein was found to effectively compete with binding by radiolabeled flg22 (IC50 = 120 nM), in microsomal fractions that presumably lack subtilases[33]. However, although flagellin can bind FLS2, it is unclear at this stage if it would also activate FLS2 signalling because that would require subsequent BAK1 binding to FLS2. The extension of flg22 at its C-terminus is likely to obstruct BAK1 binding, based on the structure of flg22 bound to the FLS2 and BAK1[34]. This indicates that proteases might be required to process flagellin whilst the flg22 epitope is protected by FLS2 (**Fig. 8**). Indeed, binding of radiolabelled flg22 to cells stabilises the peptide[33], which is consistent with the fact that the cleavage site would be obstructed upon binding FLS2[34]. This process indicates that SBT5.2 might counterbalance flagellin perception by inactivating flagellin before it is perceived, whilst also facilitating flagellin perception when it is bound to FLS2.

Although flg22 and flagellin are more stable in apoplastic fluids of *sbt5.2* plants, they are still slowly degraded. Likewise, processing of quenched peptides is significantly reduced, but not absent in apoplastic fluids of the *sbt5.2* mutant, or in apoplastic fluids from leaves expressing Epi1. These data indicate that proteases other than SBT5.2, or even Epi1-insensitive proteases, contribute to flagellin processing in the apoplast. Indeed, the apoplast contains dozens of active Ser and Cys proteases, as well as aspartic proteases (pepsins) and metalloproteases[15,35]. This suggests that the apoplast is a highly digestive microenvironment, where many proteases collectively contribute to a redundant proteolytic machinery that control levels of immunogenic peptides. The redundancy in the extracellular proteolytic machinery might explain why flagellin is still perceived in the *sbt5.2* mutant. Alternatively, flagellin processing is not required in case BAK1 can assemble with the flagellin-FLS2 complex without flagellin processing. The latter mechanism is similar to how flagellin is recognised on the cell surface receptor by TLR5 in animals[36].

We demonstrated that flg22 and flagellin immunogenicity is prolonged in *sbt5.2* mutants and that this is associated with increased antibacterial immunity when *sbt5.2* mutants are pre-treated with low flg22 concentrations (5-10 nM flg22). From a plant-centric perspective, these data indicate that SBT5.2s dampen immune responses both temporally and spatially to avoid the costly indication of antibacterial immunity in tissues that are not or no longer exposed to sufficient bacteria. From a pathogen-centric perspective, bacteria are taking advantage of the plant proteolytic machinery to avoid flg22 accumulation and detection. Relying on plant proteases rather than bacterial-secreted proteases such as AprA[37], has the advantage that flg22 immunogenicity is inactivated beyond the limits of protein diffusion. Interestingly, this mechanism may not be restricted to flagellin perception in *N. benthamiana*, as similar processing of the flg22 epitope has been detected in seedling exudates of Arabidopsis[11] and apoplastic fluids of tomato (Supplemental **Fig. S8**). This mechanism is probably also universal because the cleavage sites within the flg22 epitope are highly conserved across bacteria (Supplemental **Fig. S10**). In addition, SBT5.2a is well-conserved across plant species[18] and frequently detected in the apoplast, for instance in Arabidopsis[11]. Given its broad substrate promiscuity, SBT5.2 might be a general protease acting on diverse apoplastic proteins in various plant species, e.g. to maintain protein homeostasis in the apoplast. The role of SBT5.2 in spatial-temporal control of elicitor levels may also extend to other elicitor proteins. Indeed, we recently found that SBT5.2 is also responsible for reducing levels of csp22 epitope in Cold Shock Proteins (CSPs) of *P. syringae*[22]. Collectively, these data indicate that a conserved extracellular proteolytic machinery consisting of SBT5.2 and other proteases provides spatial-temporal control on elicitor peptide levels to restrict the induction of costly defence responses, whilst simultaneously being used by pathogens to avoid detection.

Methods

Plants materials and growth conditions - *Nicotiana benthamiana* plants were grown in a growth chamber at 22°C and ~60% relative humidity with a 16-hour photoperiod and a light intensity of 2000 cd·sr m−2.

Flagellin isolation and monomerization - *Pseudomonas syringae* bacteria were grown on LB agar plates for 24 h at 28°C. Next, bacteria were grown in 10 ml LB medium supplemented with 10 mM $MgCl_2$ for 24 h at 28°C. The culture was 1,000-fold diluted into 200 ml 10 mM $MgCl_2$ LB and grown for 48 h at 25°C. The cells were harvested by centrifugation at 5,000 x *g* for 10 min at 25°C, resuspended in 1/3 volume of minimal medium [50 mM potassium phosphate buffer, 7.6 mM $(NH_4)_2SO_4$, 1.7 mM $MgCl_2$, and 1.7 mM NaCl (pH 5.7)] supplemented with 10 mM mannitol, and then incubated for 24 h at 25°C. After centrifugation at 5,000 x *g* for 10 min at 4°C, the bacterial pellet was resuspended in 1/3 volume of ice-cold PBS pH 7.0. Bacterial flagella were sheared from the cells by vortexing for 1 min (maximum speed) and collected by centrifugation at 5,000 x *g* for 20 min at 4°C. The supernatant was filtered through a 0.45 µm filter on ice. The resultant supernatant was centrifuged at 100,000 x *g* for 2 h at 4°C. The pellet of purified flagella was suspended in 200 µl of ice-cold PBS pH 7.0. Flagella was further purified using a 100 kDa MWCO. The residues were resuspended in ice-cold PBS pH 7.0. Proteins were quantified using Qubit Fluorometric Quantification and following manufacturer's instructions (Qubit Protein BR Assay Kit, Thermo Fisher Scientific, UK). Flagella were aliquoted and used immediately or stored at - 80°C. Flagella were monomerised

by heat treatment at 70°C for 15 min. Purified flagella and flagellin proteins were separated by SDS-PAGE and stained with Coomassie.

Agroinfiltration - *Agrobacterium tumefaciens* GV3101 (pMP90) was used for agroinfiltration of *N. benthamiana*. Agrobacteria were grown overnight in Luria-Bertani (LB) medium with 10 µg/ml gentamycin and 50 µg/ml kanamycin at 28°C. For transient expression of proteins in *N. benthamiana*, overnight cultures of Agrobacterium carrying binary vectors listed in Supplemental **Table S6** were harvested by centrifugation. Bacterial cells were resuspended in agroinfiltration buffer (10 mM $MgCl_2$, 10 mM MES pH 5.6, 150 µM acetosyringone) and mixed (1:1) with agrobacteria carrying the silencing inhibitor p19 at an OD_{600} of 0.5. After 1 h at 28°C, cells were infiltrated into leaves of 4-wk-old *N. benthamiana*. The infected plants were grown in a growth chamber until use.

Quenched peptides - The quenched peptides (QPs) from flagellin were commercially synthesized with a DABCYL N-terminal modification and a Glu-EDANS C-terminal modification (GenScript, Piscataway, New Jersey, United States) at a purity of 95% (Supplemental **Table S5**). There were resuspended in DMSO at a concentration of 1 mM. This stock solution was further diluted in water to a concentration of 200 µM. AFs or purified SBT5.2a were mixed with QPs at a final concentration of 10 µM in a volume of 100 µl, and fluorescence was measured immediately at 21ºC using an Infinite M200 plate reader (Tecan, Mannedorf, Switzerland) every minute over 5 min with an excitation wavelength of 335 nm and emission wavelength of 493 nm.

Molecular cloning – Used plasmids are summarised in Supplemental **Table S6**. The binary vector encoding 35S-driven, secreted superfolded GFP with a C-terminal His-tag was produced by cloning synthetic DNA fragment (Supplemental **Table S7**) into pJK187 with Golden Gate cloning, resulting in pNS205.

Virus-induced Gene Silencing (VIGS) – Agrobacterium cultures were grown overnight and resuspended in agroinfiltration buffer at OD_{600} = 0.5. Agrobacteria carrying binary plasmids for expressing RNA2 of TRV carrying silencing fragments (Supplemental **Table S6**) were mixed 1:1 with Agrobacteria containing TRV1[38]. After incubation for 1 hour at 21°C, the mixed cultures were infiltrated into the leaves of 14-day-old *N. benthamiana* plants. The infiltrated plants were grown for another 4 to 5 weeks in a growth chamber until use.

Apoplastic Fluids (AFs) isolation - *N. benthamiana* leaves were submerged in ice-cold water and vacuum infiltrated in a 50 ml syringe with a plunger. The surface of water-infiltrated leaves was dried with absorbing paper and leaves were carefully inserted into an empty 20 ml syringe, which was placed in a 50 ml tube. AFs were collected by centrifugation at 2,000 *g* at 4°C for 10 min. AFs were immediately used or frozen using liquid nitrogen and stored at -20°C until use.

SDS-PAGE and Western blot - The protein samples were mixed with 4x gel loading buffer (200 mM Tris-HCl (pH6.8), 400 mM DTT, 8% SDS, 0.4% bromophenol blue, 40% glycerol) and heating at 90°C for 5 min. The samples were loaded on 15% SDS-PAGE and separated at 180V in Invitrogen Novex vertical gel tanks. The Amersham® Typhoon was used to measure fluorescence (Cy2: 488 nm for labelled flagellin, Cy5: 685 nm for ladder). The proteins were also visualised by total protein staining with Instant Blue® Coomassie Protein Stain (Abcam ab119211). For Western blot analysis, proteins were transferred onto a polyvinylidene

difluoride (PVDF, BioRad) membrane using BioRad Trans-blot Turbo® according to the manufacturer's instructions (BioRad Kit 1704275). Blots were blocked for 1 hours at 21°C or overnight at 4°C with 5% (w/v) skim milk in PBS-T (PBS tablets; Merck 524650, 0.1% Tween-20; Merck P1379). The membrane was incubated with 1:5000 anti-flagellin antibody[39] in 5% (w/v) skim milk for one hours at 21°C. 1:5000 anti-flagellin antibody was added in the 5% (w/v) skim milk in PBS-T for one hours at 21°C. Blots were washed twice with PBS-T for 5 minutes, and incubated with 1:5000 HRP-conjugated anti-goat antibody in PBS-T for 1 hours at 21°C. Blots were washed four times with PBS-T for 5 minutes and chemiluminescent signals were detected using Clarity Western ECL Substrate (BioRad,), and visualised using the ImageQuant® LAS-4000 imager (GE Healthcare, Healthcare Life Sciences, Little Chalfont, UK).

SBT5.2a-His purification - Four-week-old *N. benthamiana* leaves were infiltrated with a 1:1 mixture (final $OD_{600} = 0.5$ for each) of Agrobacterium tumefaciens GV3101 containing the silencing suppressor P19 and pPB097[22]. Apoplastic fluid containing SBT5.2a-His was extracted 6 days after infiltration and purified as previously described[40,41].

ROS assays - ROS assays were performed as described previously[10]. Briefly, after incubation in water overnight, one leaf disc (6 mm diameter) was added to 100 µl solution containing 25 ng/µl luminol, 25 ng/µl Horse Radish Peroxidase (HRP) and specified elicitor treatments. For assays with treated-elicitors, elicitor peptides or purified flagellin were incubated in AFs from *N. benthamiana* leaves (wild-type, agroinfiltrated, VIGS-silenced or *sbt5.2* mutants) or purified SBT5.2a-HIS for the specified time at 21°C. After incubation, 25 ng/µl luminol and 25 ng/µl HRP were added to the AFs. Chemiluminescence was measured immediately with the Infinite M200 plate reader (Tecan, Mannedorf, Switzerland) every minute for one hour. Standard errors were calculated at each time point and for each treatment.

Mass spectrometry - To generate samples for the analysis of endogenously digested peptides, 10 µg/ml of purified flagellin of *Pta*6605 or *Pta*6605Δ*fgt1* was incubated for 30 min or 60 min with apoplastic fluids isolated from leaves of *N. benthamiana*, or tomato (Money Maker Cf0), or purified SBT5.2a-HIS at 21°C (the specific condition is indicated under each figure). The samples were supplemented (AF and/or the purified proteins) with four volumes of MS-grade acetone. After incubating the mixture was kept on ice for 1 hour, and subjected to centrifugation at 18,000 x g for 20 minutes. Following centrifugation, four-fifths of the supernatants was transferred to fresh Eppendorf tubes and the acetone was evaporated using vacuum centrifugation. The dried peptide samples were sent to the Analytics Core Facility Essen (ACE) for MS analysis.

Sample clean-up for LC-MS/MS - Peptides were desalted on home-made C18 StageTips containing two layers of an octadecyl silica membrane (CDS Analytical, Oxford, PA, USA). All centrifugation steps were carried out at room temperature. The StageTips were first activated and equilibrated by passing 50 µL of methanol (600 × *g*, 2 min), 80% (v/v) acetonitrile (ACN) with 0.5% (v/v) FA (600 × *g*, 2 min) and 0.5% (v/v) FA (600 × *g*, 2 min) over the tips. Next, the acidified tryptic digests were passed over the tips (800 × *g*, 3 min). The immobilized peptides were then washed with 50 µL and 25 µL 0.5% (v/v) FA (800 × *g*, 3 min). Bound peptides were eluted from the StageTips by application of two rounds of 25 µL 80% (v/v) ACN with 0.5% (v/v) FA (800 × *g*, 2 min). After elution from the StageTips, the peptide samples were dried using a vacuum

concentrator (Eppendorf, Hamburg, Germany) and the peptides were dissolved in 15 µl 0.1% (v/v) FA prior to analysis by MS.

LC-MS/MS Analysis - LC-MS/MS analysis of peptide samples were performed on an Orbitrap Fusion Lumos mass spectrometer (Thermo Scientific, Waltham, MA, USA) coupled to a Vanquish Neo ultra high-performance liquid chromatography (UHPLC) system (Thermo Scientific, Waltham, MA, USA) or on a Thermo Orbitrap Elite mass spectrometer coupled to an Easy nLC 1000 UHPLC. Both systems were operated in the one-column mode. The analytical column was a fused silica capillary (inner diameter 75 µm, outer diameter 360 µm, length 28 – 35 cm) with an integrated sintered frit packed in-house with Kinetex 1.7 µm XB-C18 core shell material (Phenomenex, Aschaffenburg, Germany) or Reprosil-Pur 120 C18-AQ,(Dr. Maisch GmbH). The analytical column was encased by a PRSO-V2 column oven (Sonation, Biberach, Germany) and attached to a nanospray flex ion source (Thermo Scientific, Waltham, MA, USA). The column oven temperature was set to 45 – 50 °C during sample loading and data acquisition. The Vanquish Neo was equipped with two mobile phases: solvent A (2% ACN and 0.2% FA, in water) and solvent B (80% ACN and 0.2% FA, in water). The Easy nLC 100 was equipped with: solvent A (0.1% FA, in water) and solvent B (80% ACN and 0.1% FA, in water). All solvents were of UHPLC grade (Honeywell, Charlotte, NC, USA). Peptides were directly loaded onto the analytical column with a maximum flow rate that would not exceed the set pressure limit of 950 bar (usually around 0.5 – 0.6 µl min^{-1}) and separated on the analytical column by running project specific gradients. The gradient composition and the MS settings for each experiment can be found in Supplemental **Data S1**.

Peptide and Protein Identification using MaxQuant - RAW spectra were submitted to an Andromeda[42] search in MaxQuant using the default settings[43]. Label-free quantification and match-between-runs was activated[44]. The detailed search settings and which databases were used for the different experiments can be found in Supplemental **Data S1**.

Briefly, the MS/MS spectra data were searched against project specific databases. All searches included a contaminants database search (as implemented in MaxQuant, 245 entries). The contaminants database contains known MS contaminants and was included to estimate the level of contamination. Andromeda searches allowed oxidation of methionine residues (16 Da) and acetylation of the protein N-terminus (42 Da) as dynamic modifications. Enzyme specificity was set to “unspecific”. The instrument type in Andromeda searches was set to Orbitrap and the precursor mass tolerance was set to ±20 ppm (first search) and ±4.5 ppm (main search). The MS/MS match tolerance was set to ±0.5 Da. The peptide spectrum match FDR and the protein FDR were set to 0.01 (based on target-decoy approach). For protein quantification unique and razor peptides were allowed. Modified peptides were allowed for quantification. The minimum score for modified peptides was 40. Label-free protein quantification was switched on, and unique and razor peptides were considered for quantification with a minimum ratio count of 2. Retention times were recalibrated based on the built-in nonlinear time-rescaling algorithm. MS/MS identifications were transferred between LC-MS/MS runs with the “match between runs” option in which the maximal match time window was set to 0.7 min and the alignment time window set to 20 min. The quantification is based on the “value at maximum” of the extracted ion current. At least two quantitation events were required for a quantifiable protein. Further

analysis and filtering of the results was done in Perseus v1.6.10.0[45]. Comparison of protein group quantities (relative quantification) between different MS runs is based solely on the LFQ's as calculated by MaxQuant, MaxLFQ algorithm[44].

AlphaFold Multimer – All models were generated using AFM v2.1.1[32,46] on the Advanced Research Computing (ARC) clusters as described previously[41]. Briefly, the sequences of mature flagellin and SBT5.2 catalytic domain were submitted to model the structure. Database preset was set to 'full_dbs' to include the full bfd database for multi-sequence alignment search for all predictions. For flagellin monomer, 'monomer_ptm' was specified for the '--model_preset' flag to obtain pTM confidence measure. Monomer pTM score was extracted from the .pkl output file specific to the model.

Phylogenetic analysis – Flagellin sequences were collected for various Pseudomonas strains. Clustal Omega[47] was used for amino acid sequence alignment and neighbour-joining tree construction. The tree was visualised using iTOL[48] and displayed with midpoint rooting.

Activity-Based Protein Profiling (ABPP) - FP-TAMRA (Thermo-Fisher) was prepared as 10 µM stock solutions in dimethyl sulfoxide (DMSO). Serine hydrolase labelling was performed as described previously with minor modifications[49]. Briefly, apoplastic fluids were incubated with 0.2 µM FP-TAMRA (Thermo Fischer) in PBS buffer pH7 for 1h at 21°C in the dark. Labelling was stopped by adding 4 x gel loading buffer (200 mM Tris-HCl (pH 6.8), 400 mM DTT, 8% SDS, 0.4% bromophenol blue, 40% glycerol) and heating at 90°C for 5 min. The proteins were separated on SDS-PAGE and fluorescently labelled proteins were detected by in-gel scanning with the Typhoon FLA 9000 (GE Healthcare Life Sciences) using Cy3 settings (532 nm excitation and 610PB filter).

Infection assays - flg22 peptides were diluted in water. *N. benthamiana* plants were infiltrated with the different concentrations of flg22 peptide or with water as a mock control. *N. benthamiana* plants were infiltrated when 3-4 weeks-old, and 3 fully expanded leaves were infiltrated per plant. 24h later, infiltrated leaves were infiltrated with 10^5 CFU/ml *Pta*6605. The next day (1 dpi), three leaf discs were punched with a cork borer from each infected leaf, and surface-sterilised with 15% hydrogen peroxide for 2 minutes. Leaf discs were then washed twice in MilliQ and dried under sterile conditions. Leaf discs were placed into a 1.5 ml safe-lock Eppendorf tube with three 3 mm diameter metal beads and 1 ml of MilliQ. Tubes were placed in tissue lyser for five minutes at 30 Hertz/second. 200 µl of the lysed tissue was transferred to the first row (A) of a 96-well plate and then serial 10-fold dilutions were made until the last row (20 µl tissue + 180 µl MilliQ). 20 µl of undiluted tissue and serial dilutions were plated on LB-agar plates containing *Pseudomonas* CFC Agar Supplement (Oxoid SR0103). Plates were allowed to dry, incubated at 28ºC for two days and then colonies were counted. The p-value was calculated using the two-tailed Student t-test to compare bacterial growth between leaves from WT and *sbt5.2* mutant plants.

Data Availability

The mass spectrometry proteomics data for the on-bead digestions have been deposited to the ProteomeXchange Consortium via the PRIDE[50] partner repository (https://www.ebi.ac.uk/pride/archive/) with the dataset identifier PXD056369. During the review process the data can be accessed via a reviewer account

(Username: reviewer_pxd056369@ebi.ac.uk; Password: UfEybSx6pquA). Uncropped images of gels and western blots are provided as Supplemental **Data S2**.

References

1. Chevance, F. F., & Hughes, K. T. Coordinating assembly of a bacterial macromolecular machine. *Nat. Rev. Microbiol.* **6**, 455-465 (2008).

2. Gómez-Gómez, L., & Boller, T. Flagellin perception: a paradigm for innate immunity. *Trends Plant Sci.* **7**, 251-256 (2002).

3. Ramos, H. C., Rumbo, M., & Sirard, J. C. Bacterial flagellins: mediators of pathogenicity and host immune responses in mucosa. *Trends Microbiol.* **12**, 509-517 (2004).

4. Samatey, F. A., Imada, K., Nagashima, S., Vonderviszt, F., Kumasaka, T., Yamamoto, M., & Namba, K. Structure of the bacterial flagellar protofilament and implications for a switch for supercoiling. *Nature* **410**, 331-337 (2001).

5. Chiku, K., Yamamoto, M., Ohnishi-Kameyama, M., Ishii, T., Yoshida, M., Taguchi, F., Ichinose, Y., & Ono, H. Comparative analysis of flagellin glycans among pathovars of phytopathogenic *Pseudomonas syringae*. *Carbohydr. Res.* **375**, 100-104 (2013).

6. Gómez-Gómez, L., & Boller, T. FLS2: an LRR receptor-like kinase involved in the perception of the bacterial elicitor flagellin in Arabidopsis. *Mol Cell.* 5, 1003-1011 (2000).

7. Felix, G., Duran, J. D., Volko, S., & Boller T. (1999) Plants have a sensitive perception system for the most conserved domain of bacterial flagellin. *Plant J.* **18**, 265-276 (1999).

8. Zipfel, C., Robatzek, S., Navarro, L., Oakeley, E. J., Jones, J. D. G., Felix, G., & Boller, T. Bacterial disease resistance in Arabidopsis through flagellin perception. *Nature* **428**, 764-767 (2004).

9. Chen, C., van der Hoorn, R. A. L, & Buscaill, P. Releasing hidden MAMPs from precursor proteins in plants. *Trends Plant Sci.* **29**, 428-436 (2024).

10. Buscaill, P., Chandrasekar, B., Sanguankiattichai, N., Kourelis, J., Kaschani, F., Thomas, E. L., Morimoto, K., Kaiser, M., Preston, G. M., Ichinose, Y., van der Hoorn, R. A. L. Glycosidase and glycan polymorphism control hydrolytic release of immunogenic flagellin peptides. *Science* **364**, eaav0748 (2019).

11. Matsui, S., Noda, S., Kuwata, K., Nomoto, M., Tada, Y., Shinohara, H., & Matsubayashi, Y. Arabidopsis SBT5.2 and SBT1.7 subtilases mediate C-terminal cleavage of flg22 epitope from bacterial flagellin. *Nat. Commun.* **15**, 3762 (2024).

12. Wu, L., Xiao, H., Zhao, L., & Cheng, Q. CRISPR/Cas9-mediated generation of fls2 mutant in *Nicotiana benthamiana* for investigating the flagellin recognition spectrum of diverse FLS2 receptors. *Plant Biotechnol J.* **20**, 1853-1855 (2022).

13. Taguchi, F., Takeuchi, K., Katoh, E., Murata, K., Suzuki, T., Marutani, M., Kawasaki, T., Eguchi, M., Katoh, S., Kaku, H., Yasuda, C., Inagaki, Y., Toyoda, K., Shiraishi, T., & Ichinose, Y. Identification of glycosylation genes and glycosylated amino acids of flagellin in *Pseudomonas syringae* pv. *tabaci*. *Cell Microbiol.* **8**, 923-938 (2006).

14. Tian, M., Huitema, E., Da Cunha, L., Torto-Alalibo, T., & Kamoun, S. A Kazal-like extracellular serine protease inhibitor from *Phytophthora infestans* targets the tomato pathogenesis-related protease P69B. *J. Biol. Chem.* **279**, 26370-26377 (2004).
15. Jutras, P. V., Grosse-Holz, F., Kaschani, F., Kaiser, M., Michaud, D., & van der Hoorn, R. A. L. Activity-based proteomics reveals nine target proteases for the recombinant protein-stabilizing inhibitor SlCYS8 in *Nicotiana benthamiana*. *Plant Biotechnol J.* **17**, 1670-1678 (2019).
16. Grosse-Holz, F., Madeira, L., Zahid, M. A., Songer, M., Kourelis, J., Fesenko, M., Ninck, S., Kaschani, F., Kaiser, M., & van der Hoorn, R. A. L. Three unrelated protease inhibitors enhance accumulation of pharmaceutical recombinant proteins in *Nicotiana benthamiana. Plant Biotechnol. J.* **16**, 1797-1810 (2018).
17. Kourelis, J., Kaschani, F., Grosse-Holz, F. M., Homma, F., Kaiser, M., & van der Hoorn, R. A. L. A homology-guided, genome-based proteome for improved proteomics in the alloploid *Nicotiana benthamiana*. *BMC Genomics* **20**, 722 (2019).
18. Beritza, K., Buscaill, P., Song, S., Jutras, P. V., Huang, J., Mach, L., Dong, S., & Van der Hoorn, R. A. L. SBT5.2s are the major active extracellular subtilases processing IgG antibody 2F5 in the *N. benthamiana* apoplast. *Plant Biotechn. J. in press* (2024).
19. Sueldo, D. J., Godson, A., Kaschani, F., Krahn, D., Kessenbrock, T., Buscaill, P., Schofield, C. J., Kaiser, M., & van der Hoorn, R. A. L. Activity-based proteomics uncovers suppressed hydrolases and a neo-functionalised antibacterial enzyme at the plant-pathogen interface. *New Phytol.* **241**, 394-408 (2024).
20. Puchol Tarazona, A. A., Maresch, D., Grill, A., Bakalarz, J., Torres Acosta, J. A., Castilho, A., Steinkellner, H., & Mach, L. Identification of two subtilisin-like serine proteases engaged in the degradation of recombinant proteins in *Nicotiana benthamiana*. *FEBS Lett*. **595**, 379-388 (2021).
21. Reichardt, S., Repper, D., Tuzhikov, A. I., Galiullina, R. A., Planas-Marquès, M., Chichkova, N. V., Vartapetian, A. B., Stintzi, A., & Schaller, A. The tomato subtilase family includes several cell death-related proteinases with caspase specificity. *Sci. Rep.* **8** 10531 (2018).
22. Chen, C., Buscaill, P., Sanguankiattichai, N., Huang, J., Kaschani, F., Kaiser, M., & Van der Hoorn, R. A. L. Extracellular plant subtilases dampen cold shock peptide elicitor levels. *Nat. Plants in press* (2024).
23. Tsuda, K., Sato, M., Stoddard, T., Glazebrook, J., & Katagiri, F. Network properties of robust immunity in plants. *PLoS Genet.* **5**, e1000772 (2009).
24. Auvray, F., Thomas, J., Fraser, G. M., & Hughes, C. Flagellin polymerisation control by a cytosolic export chaperone. *J Mol Biol.* **308**, 221-229 (2001).
25. Felix, G., & Boller, T. Molecular sensing of bacteria in plants. The highly conserved RNA-binding motif RNP-1 of bacterial cold shock proteins is recognized as an elicitor signal in tobacco. *J Biol Chem.* **278**, 6201-6208 (2002).
25. Kunze, G., Zipfel, C., Robatzek, S., Niehaus, K., Boller, T., & Felix, G. The N terminus of bacterial elongation factor Tu elicits innate immunity in Arabidopsis plants. *Plant Cell* **16**, 3496-3507 (2004).
26. Yonekura, K., Maki, S., Morgan, D. G., DeRosier, D. J., Vonderviszt, F., Imada. K., & Namba, K. The bacterial flagellar cap as the rotary promoter of flagellin self-assembly. *Science* 290, 2148-2152 (2000).

27. Shimizu, R., Taguchi, F., Marutani, M., Mukaihara, T., Inagaki, Y., Toyoda, K., Shiraishi, T., & Ichinose, Y. The DeltafliD mutant of *Pseudomonas syringae* pv. *tabaci*, which secretes flagellin monomers, induces a strong hypersensitive reaction (HR) in non-host tomato cells. *Mol Genet Genomics.* **269**, 21-30 (2003).
28. Zhu, S., & Gao, B. Bacterial flagella loss under starvation. *Trends Microbiol.* 28, 785-788 (2020).
29. Kint, N., & Viollier, P. H. (2023) Extracellular transfer of a conserved polymerization factor for multi-flagellin filament assembly in Caulobacter. *Cell Rep.* **42**, 112890 (2023).
30. Kostyukova, A. S., Pyatibratov, M. G., Filimonov, V. V., & Fedorov, O. V. Flagellin parts acquiring a regular structure during polymerization are disposed on the molecule ends. *FEBS Lett.* **241**, 141-144 (1988).
31. Aizawa, S. I., Vonderviszt, F., Ishima, R., & Akasaka, K. Termini of Salmonella flagellin are disordered and become organized upon polymerization into flagellar filament. *J. Mol. Biol.* **211**, 673-677 (1990).
32. Evans, R., O'Neill, M., Pritzel, A., Antropova, N., Senior, A., Green, T., Žídek, A., Bates, R., Blackwell, S., Yim, J., Ronneberger, O., Bodenstein, S., Zielinski, M., Bridgland, A., Potapenko, A., Cowie, A., Tunyasuvunakool, K., Jain, R., Clancy, E., Kohli, P., Jumper, J., & Hassabis, D. Protein complex prediction with AlphaFold-Multimer. *bioRxiv* 2021.10.04.463034 (2021).
33. Meindl, T., Boller, T., & Felix, G. The bacterial elicitor flagellin activates its receptor in tomato cells according to the address-message concept. *Plant Cell* **12**, 1783-1794 (2000).
34. Sun, Y., Li, L., Macho, A. P., Han, Z., Hu, Z., Zipfel, C., Zhou, J. M., & Chai, J. Structural basis for flg22-induced activation of the Arabidopsis FLS2-BAK1 immune complex. *Science* **342**, 624-628 (2013).
35. Grosse-Holz, F., Kelly, S., Blaskowski, S., Kaschani, F., Kaiser, M., & van der Hoorn, R. A. L. (2018a) The transcriptome, extracellular proteome and active secretome of agroinfiltrated *Nicotiana benthamiana* uncover a large, diverse protease repertoire. *Plant Biotechnol J.* **16**, 1068-1084 (2018).
36. Yoon, S. I., Kurnasov, O., Natarajan, V., Hong, M., Gudkov, A. V., Osterman, A. L., & Wilson, I. A. Structural basis of TLR5-flagellin recognition and signaling. *Science* 335, 859-864 (2012).
37. Pel, M. J., van Dijken, A. J., Bardoel, B. W., Seidl, M. F., van der Ent, S., van Strijp, J. A., & Pieterse, C. M. *Pseudomonas syringae* evades host immunity by degrading flagellin monomers with alkaline protease AprA. *Mol. Plant Microbe Interact.* **27**, 603-610 (2014).
38. Liu, Y., Schiff, M., & Dinesh-Kumar, S. P. Virus-induced gene silencing in tomato. *Plant J.* **31**, 777-786 (2002).
39. Taguchi, F., Shimizu, R., Nakajima, R., Toyoda, K., Shiraishi, T., & Ichinose, Y. Differential effects of flagellins from *Pseudomonas syringae* pv. *tabaci*, *tomato* and *glycinea* on plant defense response. *Plant Physiol. Biochem.* **41**, 165-174 (2003).
40. Schuster, M., Eisele, S., Armas-Egas, L., Kessenbrock, T., Kourelis, J., Kaiser, M., & van der Hoorn, R. A. L. Enhanced late blight resistance by engineering an EpiC2B-insensitive immune protease. *Plant Biotechnol J.* **22**, 284-286 (2024).
41. Homma, F., Huang, J., & van der Hoorn, R. A. L. AlphaFold-Multimer predicts cross-kingdom interactions at the plant-pathogen interface. *Nat Commun.* **14**, 6040 (2023).
42. Cox, J., Neuhauser, N., Michalski, A., Scheltema, R. A., Olsen, J. V. & Mann, M. Andromeda: a peptide search engine integrated into the MaxQuant environment. *J Proteome Res.* **10**, 1794-1805 (2011).

43. Cox, J. & Mann, M. MaxQuant enables high peptide identification rates, individualized p.p.b.-range mass accuracies and proteome-wide protein quantification. *Nat Biotechnol*. **26**, 1367-1372 (2008).
44. Cox, J., Hein, M. Y., Luber, C. A., Paron, I., Nagaraj, N. & Mann, M. (2014) Accurate proteome-wide label-free quantification by delayed normalization and maximal peptide ratio extraction, termed MaxLFQ. *Mol Cell Proteomics.* **13**, 2513-2526 (2014).
45. Tyanova, S., Temu, T., Sinitcyn, P., Carlson, A., Hein, M. Y., Geiger, T., Mann, M. & Cox, J. The Perseus computational platform for comprehensive analysis of (prote)omics data. *Nat Methods.* **13**, 731-740 (2016).
46. Jumper, J., Evans, R., Pritzel, A., Green, T., Figurnov, M., Ronneberger, O., Tunyasuvunakool, K., Bates, R., Žídek, A., Potapenko, A., Bridgland, A., Meyer, C., Kohl, S. A. A., Ballard, A. J., Cowie, A., Romera-Paredes, B., Nikolov, S., Jain, R., Adler, J., Back, T., Petersen, S., Reiman, D., Clancy, E., Zielinski, M., Steinegger, M., Pacholska, M., Berghammer, T., Bodenstein, S., Silver, D., Vinyals, O., Senior, A. W., Kavukcuoglu, K., Kohli, P., & Hassabis, D. Highly accurate protein structure prediction with AlphaFold. *Nature* **596**, 583-589 (2021).
47. Sievers, F., & Higgins, D. G. Clustal Omega for making accurate alignments of many protein sequences. *Protein Sci.* **27**, 135-145 (2018).
48. Letunic, I., & Bork, P. Interactive Tree of Life (iTOL) v6: recent updates to the phylogenetic tree display and annotation tool. *Nucleic Acids Res.* **13**, gkae268 (2024).
49. Kaschani, F., Gu, C., Niessen, S., Hoover, H., Cravatt, B. F., & van der Hoorn, R. A. L. (2009) Diversity of serine hydrolase activities of unchallenged and botrytis-infected *Arabidopsis thaliana*. *Mol. Cell. Proteomics* **8**, 1082-1093 (2009).
50. Vizcaíno, J. A., Csordas, A., Del-Toro, N., Dianes, J. A., Griss, J., Lavidas, I., Mayer, G., Perez-Riverol, Y., Reisinger, F., Ternent, T., Xu, Q. W., Wang, R. & Hermjakob, H. 2016 update of the PRIDE database and its related tools. *Nucleic Acids Res.* **44**, 11033 (2016).

Acknowledgements

We like to thank Ben Excel for his help with purifying flagellin; Yuki Ichinose for providing the anti-flagellin antibody; Qiang Cheng for providing the *fls2* mutant, Urszula Pyzio for excellent plant care; and Sarah Rodgers, Patricia Bowman and Caroline O'Brien for excellent technical support. This project was financially supported by BBSRC 17RM3 project BB/R017913/3 'GH35' (PB) and 19RM3 project BB/015128/1 'Galactosyrin' (PB, NS); ERC-2020-AdG project 101019324 'ExtraImmune' (JH, BM, RH); BBSRC Interdisciplinary Bioscience DTP project DDT00230 (JL); the National Natural Science Foundation of China (No. 32070289 to YL) and the Chinese Academy of Sciences Scholarship (YL).

Author contributions

PB and RH conceived the project; PB performed most of the experiments with help of NS, JH and BM; FK and MK performed proteomic analysis; PB and JH performed experiments with purified SBT5.2; PB and DS

analysed susceptibility of *TRV::SBT5.2* plants; JL produced AlphaFold Multimer models; PB and YL performed bacterial growth assays on *sbt5.2* plants; PB and RH wrote the manuscript with input of all authors.

Competing interests

The authors declare no competing interests.

FIGURES

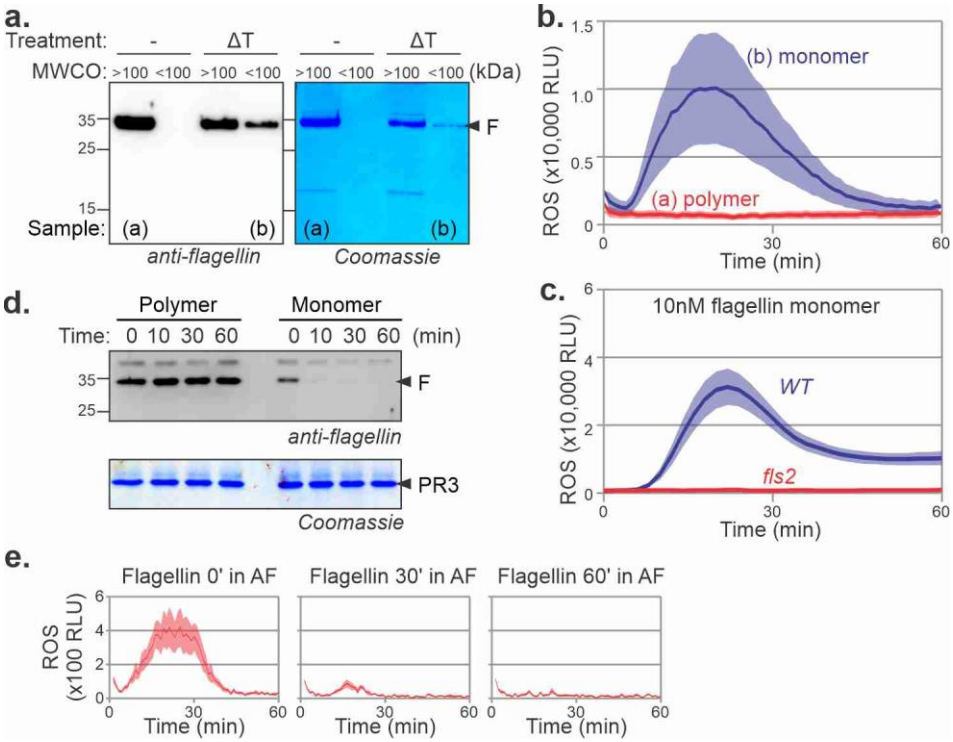

Fig. 1. Monomeric flagellin is recognised and quickly inactivated extracellularly.

a. Flagellin monomerisation. Purified flagellin from *Pta*6605 bacteria was treated with/without heat (10' 70°C, ΔT) and both samples were centrifugated through a 100 kDa MW cut-off filter. The flow-through (<100 kDa) and the residue (>100 kDa) for each sample was incubated for 30 min and separated on 15% SDS-PAGE and stained with Coomassie or analysed by western blotting using anti-flagellin antibodies. **b.** Monomeric but not polymeric flagellin is recognised in *N. benthamiana*. Leaf discs of wild-type *N. benthamiana* floating on a solution containing luminol and horse radish peroxidase (HRP) were incubated with 10 µg/mL flagellin proteins (samples a and b from Figure 1a) and the luminescence was measured over time. Error shades represent the SE of n=6 replicates. RLU, relative luminescence units. **c.** Mutant *fls2* is not responding to monomerised flagellin. Leaf discs of wild-type and *fls2* mutant *N. benthamiana* floating on a solution containing luminol and horse radish peroxidase (HRP) were incubated with 10 µg/mL monomerised flagellin and the luminescence was measured over time. Error shades represent the SE of n=6 replicates. RLU, relative luminescence units. **d.** Monomeric flagellin but not polymeric flagellin is quickly degraded in the apoplast of *N. benthamiana*. Purified polymeric flagellin was monomerised by heat treatment and incubated with apoplastic fluids (AF) isolated from *N. benthamiana* leaves for 0, 10, 30 and 60 minutes and analysed by western blot using anti-flagellin antibodies and by Coomassie staining. Pathogenesis related-3 (PR3) is an abundant apoplastic protein and served here as a loading control. **e.** Monomerised flagellin is quickly inactivated in AF. 10 µg/ml monomeric flagellin was incubated with AF for 0, 30 or 60 minutes and treated samples were added to leaf discs floating on luminol-HRP and ROS release was monitored using a luminescence plate reader for 60 minutes. Error shades represent SE of n=6 biological replicates. RLU, relative luminescence units.

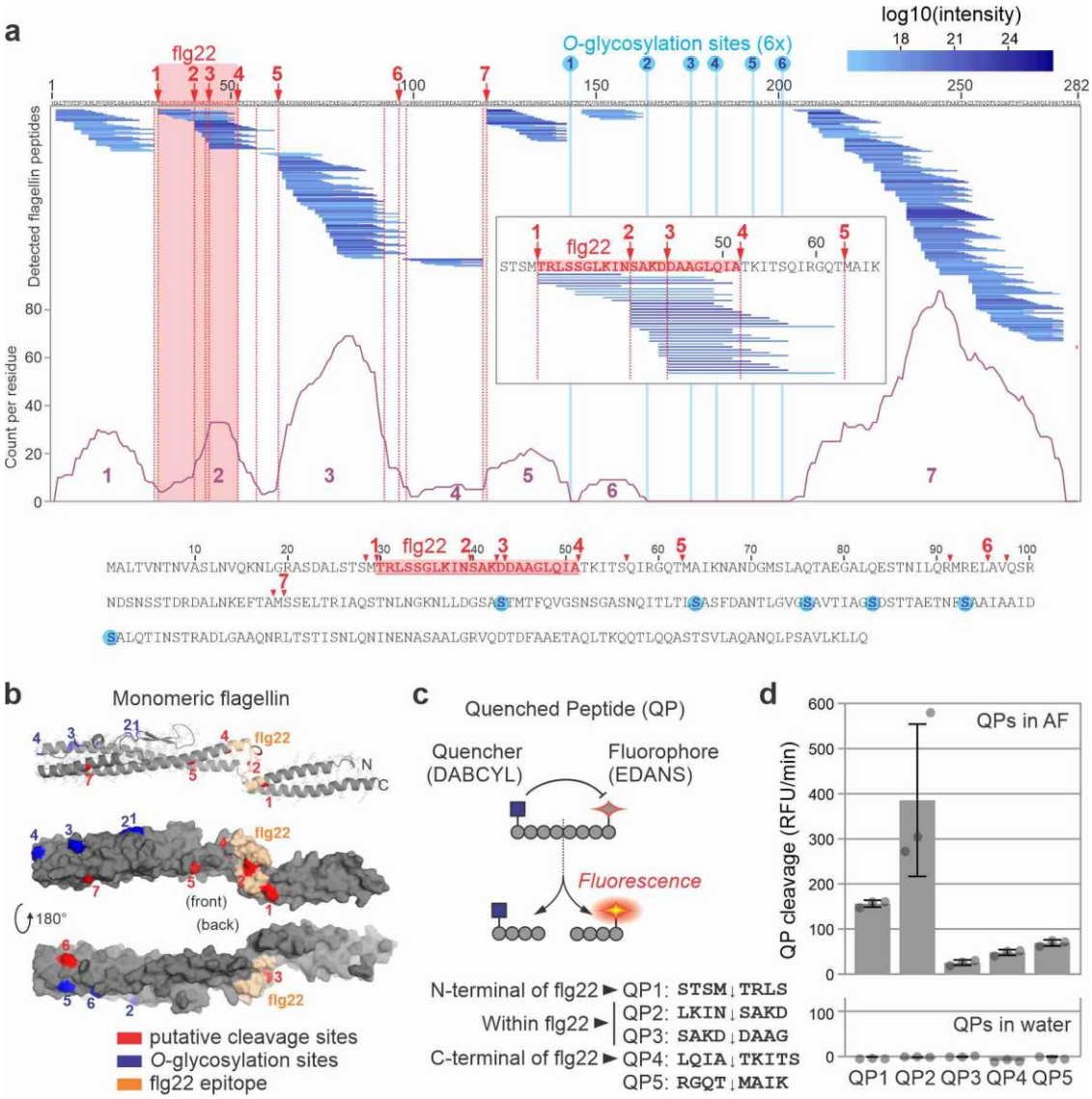

Fig. 2 Flagellin is degraded by apoplastic proteases.

a. Degradation products of flagellin in AF detected by LC-MS/MS analysis. Purified flagellin was incubated with AF isolated from *N. benthamiana* leaves. Proteins were precipitated with 80% acetone and the supernatant (peptide fraction) was analysed by LC-MS/MS. Flagellin-derived peptides were matched to the flagellin protein sequence. Highlighted are the flg22 sequence (grey), putative cleavage sites (red dashed lines) and six *O*-glycosylation sites (light blue lines). The number of times each residue was detected in the peptides is indicated with the purple graph, showing the peptides align in seven clusters. Below: position of the putative cleavage sites within the flagellin protein sequence. Highlighted are flg22 (grey), putative cleavage sites (red) and the six *O*-glycosylation sites (blue). Inset: region containing flg22 and cleavage sites 1-5 with the corresponding detected peptides. **b.** Location of putative cleavage sites within the predicted structure of the flagellin monomer, generated with AlphaFold. Highlighted are the putative cleavage sites (red), and the *O*-glycosylation sites (blue). **c.** Concept of using quenched peptides (QPs) to monitor processing. QP cleavage separates the fluorophore from the quencher, resulting in fluorescence. Five QPs containing the cleavage regions in flagellin were custom-synthesised. **d.** All QPs are processed in AF but with different efficiencies. QPs were mixed with water or AF and fluorescence was measured immediately over 5 min. Error bars represent SE of n=3 different AFs.

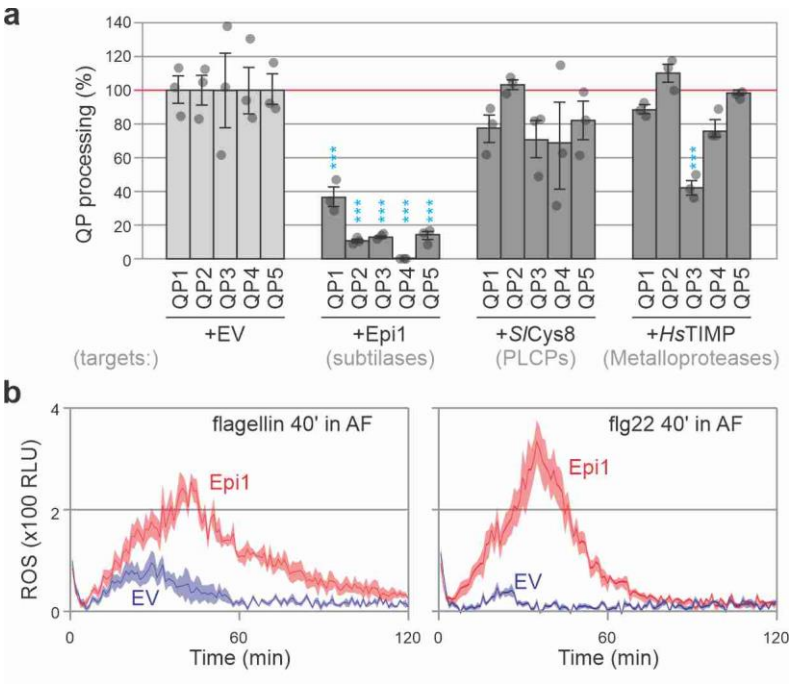

Fig. 3. Subtilase-inhibitor Epi1 suppresses processing of Qps, flg22 and flagellin.

a. Subtilase inhibitor Epi1 suppresses processing of all quenched peptides (QPs). Apoplastic fluids (AFs) isolated from *N. benthamiana* leaves transiently expressing protease inhibitors Epi1, *Sl*Cys8 and *Hs*TIMP were mixed with QPs and fluorescence and was immediately monitored using a plate. QP processing in the empty vector (EV) control was set at 100% for each QP. Error bars represent ±SE of n = 3 biological replicates (i.e., AFs from 3 plants). Students *t*-test: *, $p<0.05$; **, $p<0.01$; ***, $p<0.001$. **b.** Epi1 increases immunogenicity of monomeric flagellin and flg22. AFs from plants transiently expressing Epi1 or the empty vector (EV) control were incubated with 10 µg/ml monomeric flagellin or 100 nM flg22 for 40 min and then added to leaf discs of *N. benthamiana* plants floating on luminol and horse radish peroxidase (HRP). ROS release was measured for 120 minutes by luminescence (relative light units, RLU) using a plate reader. Error shades represent SE of n=6 replicates. RLU, relative luminescence units.

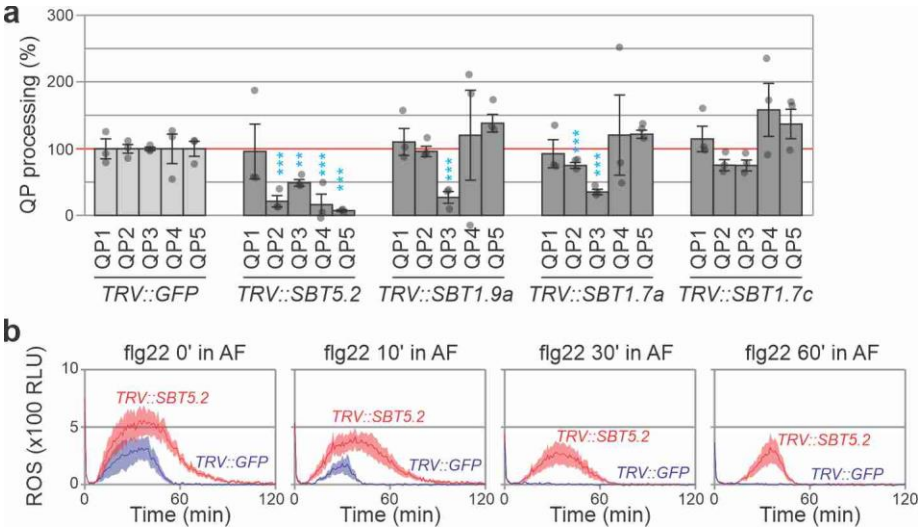

Fig. 4. SBT5.2 is required for processing QPs 2-5 and inactivating flg22.

a. SBT5.2 is required for QP processing in AF. AF from plants silenced for various subtilases were mixed with 10 µM quenched peptides and fluorescence was monitored immediately using a plate reader. QP processing in AF of *TRV::GFP* control plants was set at 100%. Error bars represent SE of n=3 different plants. Students *t*-test: *, $p<0.05$; **, $p<0.01$; ***, $p<0.001$. Please note that due to variation in silencing efficiency and the low number of replicates, QP1 processing in *TRV::SBT5.2* plants might be disturbed by an outlier, and the significance of reduced QP2 processing in SBT1.7a plants may not be relevant. **b.** *SBT5.2* silencing reduces the degradation of flg22 immunogenicity. 100 nM flg22 was incubated in AF from *TRV::SBT5.2* or *TRV::GFP* plants for 0, 30 and 60 minutes before adding to leaf discs from *N. benthamiana* floating in HRP or luminol. Luminescence was measured and plotted against time. Error shades indicate SE of n=6 replicates. RLU, relative luminescence units.

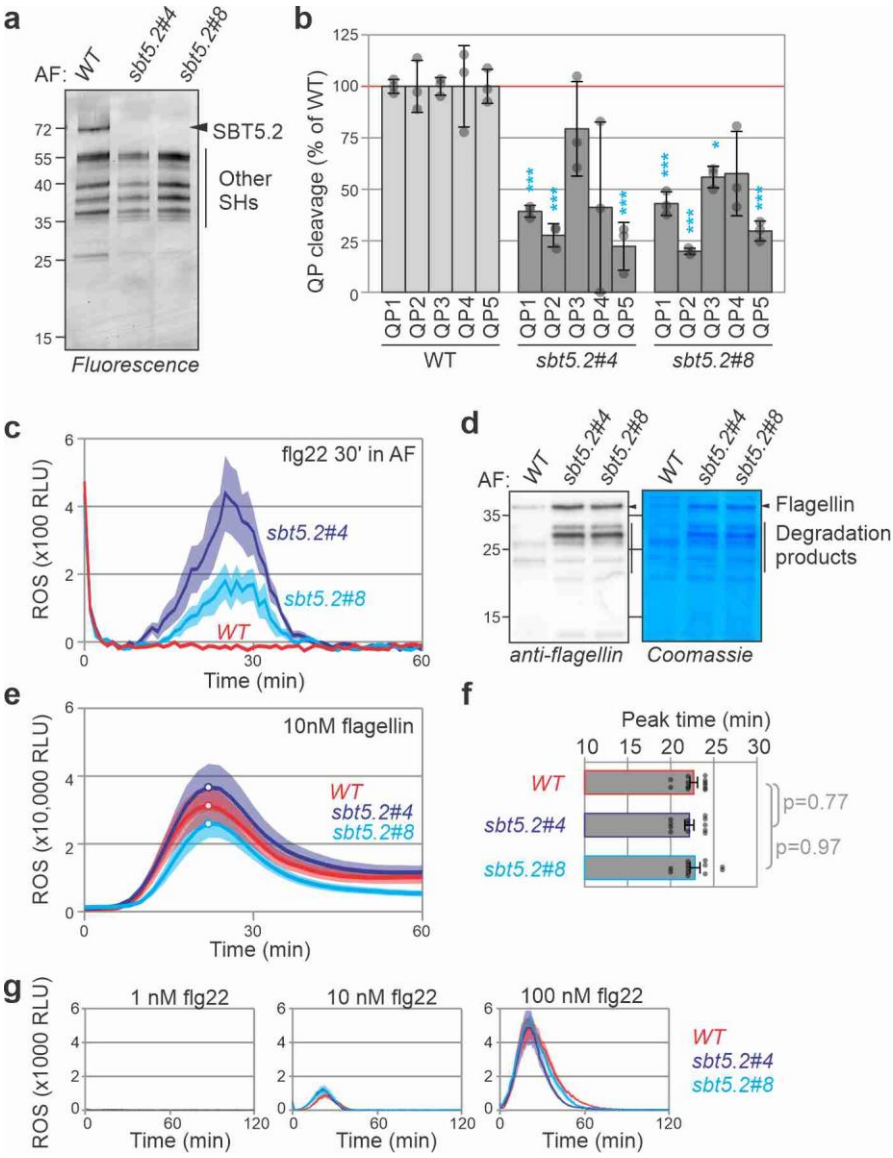

Fig. 5 *sbt5.2* mutants show reduced flagellin, flg22 and processing of quenched peptides.

a. SBT5.2s are the major active subtilases in the apoplast. AF was isolated from WT plants and two triple *sbt5.2* mutants and serine hydrolases (SHs) were labelled with FP-TAMRA and detected by in-gel fluorescence scanning. **b.** QP processing is reduced in AF isolated from both *sbt5.2* triple mutants. 10 µM QPs were incubated with AF of WT or *sbt5.2* mutants and fluorescence was measured with a plate reader. Error bars represent SE of n=4 samples. Students *t*-test: *, p<0.05; **, p<0.01; ***, p<0.001. **c.** flg22 inactivation is reduced in AF isolated from both *sbt5.2* triple mutants. AF from leaves of WT or *sbt5.2* mutant plants were incubated with 100 nM flg22 peptide for 30 minutes then added to *N. benthamiana* leaf discs floating on luminol-HRP solution. The ROS burst was monitored using a luminescence plate reader. Error shades represent SE of n=6 biological replicates. RLU, relative luminescence units. **d.** Reduced flagellin processing in the *sbt5.2* mutants. Purified flagellin was incubated for 30 min with AF from leaves of WT or *sbt5.2* mutants. The samples were separated on SDS-PAGE and stained with Coomassie or analysed by western blotting using anti-flagellin antibodies. **e.** Timing of the oxidative burst upon flagellin recognition is indistinguishable between WT plants and *sbt5.2* mutants. 10 nM flg22 was added to *N. benthamiana* leaf discs floating on luminol-HRP solution. The ROS burst was monitored using a luminescence plate reader. Error shades

represent SE of n=12 biological replicates. RLU, relative luminescence units. **f.** Peak times taken from (e) are not different between WT and *sbt5.2* mutants. Error bars represent SE of n=12 replicates and p values were calculated with ANOVA by Tukey HSD test. **g.** No altered response to flg22 in *sbt5.2* mutants. Leaf discs from 4-week-old *N. benthamiana* WT or *sbt5.2* mutants floating on luminal-HRP were treated with 1, 10 or 100 nM flg22 and ROS burst was monitored using a plate reader. Error shades represent SE of n=6 biological replicates.

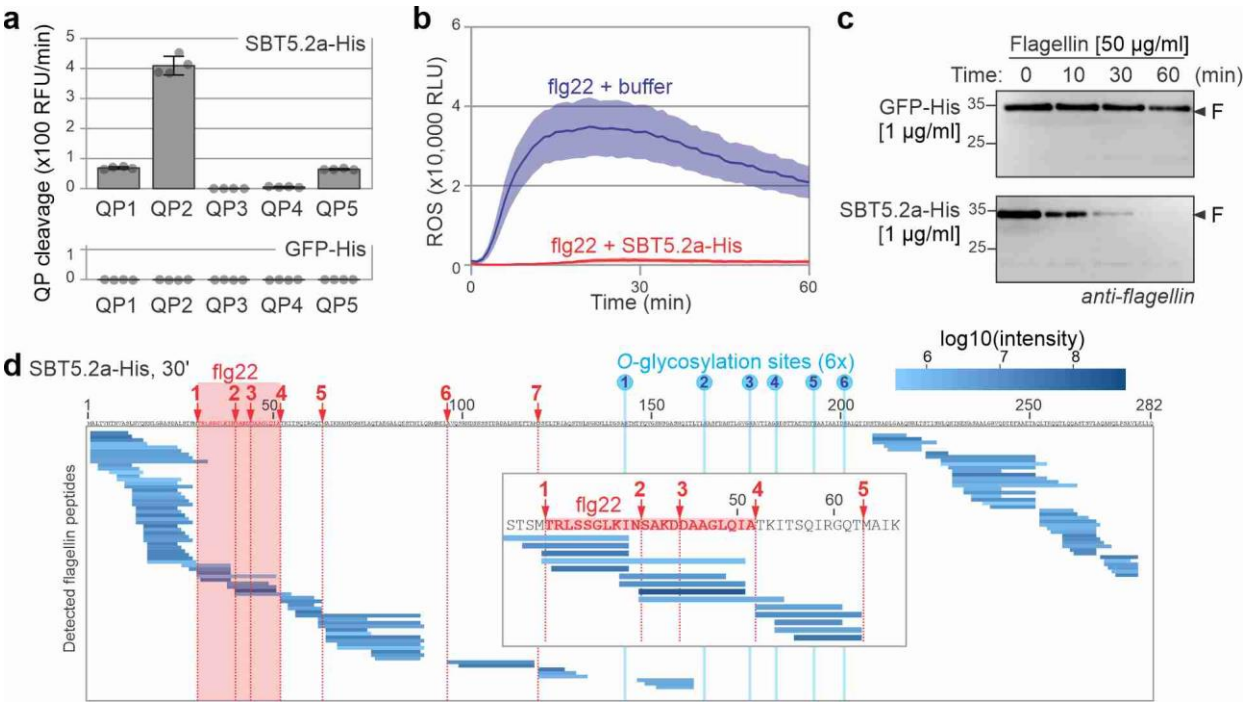

Fig. 6. Purified SBT5.2a degrades flagellin and inactivates flg22.

a. Purified SBT5.2a-His cleaves QPs. QPs were incubated with 10 µl of 25 µg/ml purified SBT5.2a-His or GFP-His and fluorescence was measured. Error bars represent SE of n=4 replicates. **b.** Purified SBT5.2a-His inactivates the flg22 elicitor. 50 nM flg22 was incubated with various concentrations of purified SBT5.2a-His for 40 minutes. These samples were added to leaf discs of *N. benthamiana* plants floating on luminol-HRP solution and the ROS burst was monitored using a luminescence plate reader. Error shades represent SE of n=6 biological replicates. RLU, relative luminescence units. **c.** Purified SBT5.2a-His quickly processes flagellin. Purified flagellin (50 µg/ml) was incubated with of purified SBT5.2a-His or GFP-His (1 µg/ml) for 0, 10, 30 or 60 minutes and samples were separated on SDS-PAGE and stained with Coomassie or analysed by western blotting using anti-flagellin antibodies. **d.** Purified SBT5.2a-His cleaves flagellin in the flg22 epitope. Flagellin was incubated with purified SBT5.2-His for 30 minutes and the released peptides were analysed by LC-MS/MS. Shown is the mean of n=3 replicates.

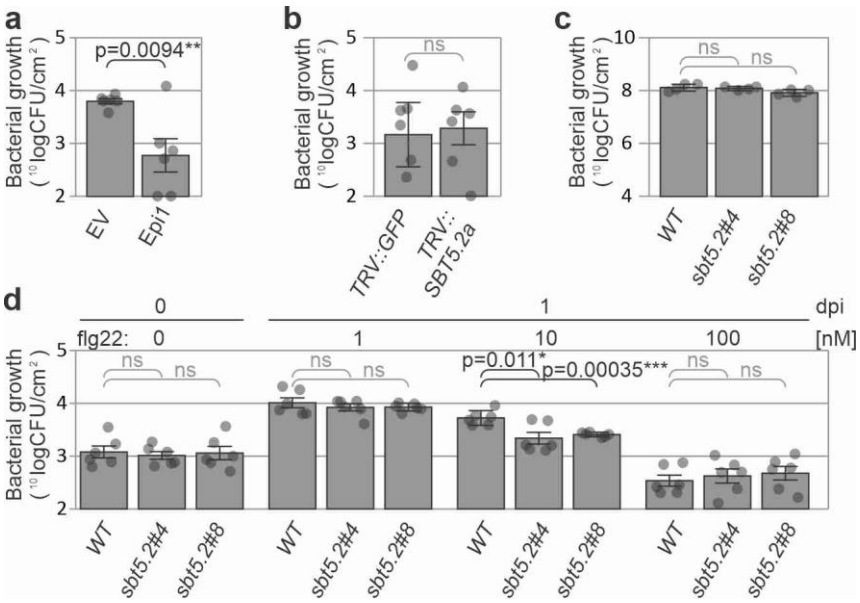

Fig. 7 SBT5.2s dampens elicitor levels to reduce antibacterial immunity.

a. Increased antibacterial immunity in leaves transiently expressing Epi1. Agroinfiltrated leaves expressing empty vector (EV) or Epi1 were sprayed with *Pta*6605 at day-3 post agroinfiltration and bacterial growth was measured three days later. Error bars represent SE of n=6 biological replicates. The p-value was calculated using the two-tailed Student t-test. **b.** No altered susceptibility *SBT5.2* silenced plants to *Pta*6605. *TRV::GFP* and *TRV::SBT5.2* plants were spray-infected with *Pta*6605 and bacterial growth was determined at 3dpi. Error bars represent SE of n=3 biological replicates. **c.** No altered susceptibility of *sbt5.2* plants to *Pto*DC3000(*ΔhQ*). Plants were spray inoculated with *Pto*DC3000(*ΔhQ*) and bacterial growth was determined at 3dpi. Error bars represent STDEV of n=4 replicates. **d.** Immune priming by low flg22 concentrations increases in *sbt5.2* mutant plants. Leaves of 4-week-old WT and *sbt5.2* mutant plants were infiltrated with 1, 10 or 100 nM flg22 or water. After 24 hours incubation, the leaves were infiltrated with $1x10^5$ bacteria/ml *Pta*6605. Colony forming units (CFUs) were determined one day post infection (dpi). Error bars represent SE of n=6 replicates.

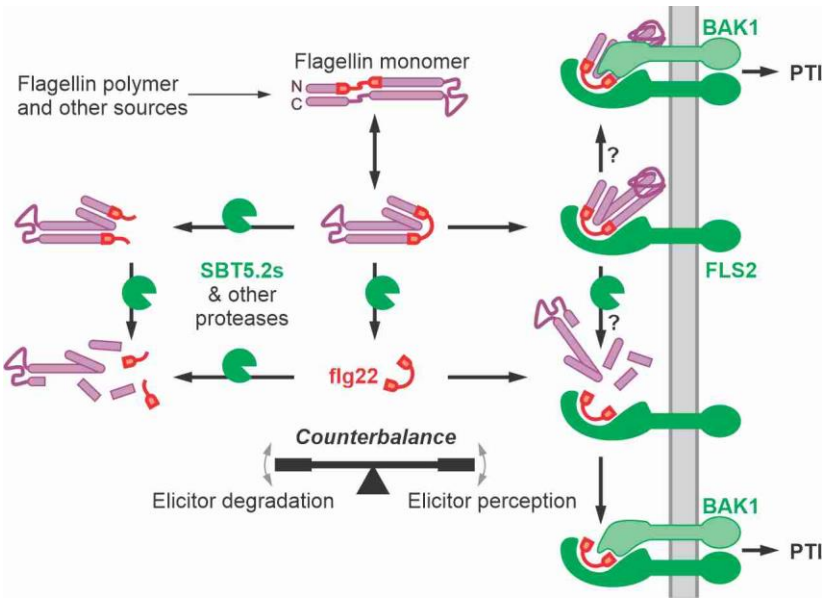

Fig. 8 SBT5.2 counterbalances elicitor perception and inactivation.

Elicitor activity of both flagellin and flg22 is quickly inactivated by SBT5.2s and other proteases cleaving in the middle of the flg22 epitope, yet sufficient flg22 may be released and bind FLS2. Flagellin protein can bind to FLS2 and may associate with BAK1 to trigger immunity without requiring processing. Alternatively, FLS2 may stabilise the flg22 epitope by binding flagellin and SBT5.2s and other proteases may process flagellin to facilitate BAK1 association and subsequent immune signalling. PTI, pattern-triggered immunity; PM, plasma membrane.